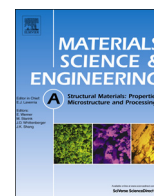




ELSEVIER

Contents lists available at ScienceDirect

## Materials Science &amp; Engineering A

journal homepage: [www.elsevier.com/locate/msea](http://www.elsevier.com/locate/msea)

## Anomalous multiple pop-in behavior in Cu–Sn-based intermetallic compounds during nanoindentation

Hoin Jun<sup>a</sup>, Yiseol Kim<sup>b</sup>, Sangjun Lee<sup>b</sup>, Namhyun Kang<sup>b,c</sup>, Kyoung-Bo Kim<sup>d</sup>, Moojin Kim<sup>d</sup>, Soo Hyung Kim<sup>b,e</sup>, Dongyun Lee<sup>b,f,\*</sup><sup>a</sup> ACI Plating Group, Samsung Electro Mechanics, 333, Noksansaneopjung-ro, Gangseo-gu, Busan 618-721, Republic of Korea<sup>b</sup> Department of Advanced Circuit Interconnection, Pusan National University, Busan 609-735, Republic of Korea<sup>c</sup> School of Materials Science and Engineering, Pusan National University, Busan 609-735, Republic of Korea<sup>d</sup> POSCO Technical Research Laboratories, Songdo-dong, Yeonsu-gu, Incheon-si 406-840, Republic of Korea<sup>e</sup> Department of Nano Fusion Technology, Pusan National University, Busan 609-735, Republic of Korea<sup>f</sup> Department of Cogno-Mechatronics Engineering, Pusan National University, Busan 609-735, Republic of Korea

## ARTICLE INFO

## Article history:

Received 14 February 2014

Received in revised form

17 April 2014

Accepted 14 June 2014

Available online 20 June 2014

## Keywords:

Intermetallic compounds

Pop-in

Dislocations

Nanoindentation

## ABSTRACT

Mechanical properties of binary intermetallic compounds (IMCs) on Sn-based solder ( $\text{Cu}_6\text{Sn}_5$  and  $\text{Cu}_3\text{Sn}$ ) on the interface between the solder alloy and its bonding pads by nanoindentation are examined.  $\text{Cu}_6\text{Sn}_5$  and  $\text{Cu}_3\text{Sn}$  binary IMCs are intentionally formed in between Sn and Cu plates. A Cu–Sn diffusion couple was prepared and annealed at 325 °C for 48 h in an Ar atmosphere. While the elastic modulus of  $\text{Cu}_3\text{Sn}$  (~140 GPa) was about 12% higher than that of  $\text{Cu}_6\text{Sn}_5$  (~125 GPa) at 0.05 s<sup>-1</sup>, the hardness of  $\text{Cu}_3\text{Sn}$  (~6 GPa) was about 15% lower than that of  $\text{Cu}_6\text{Sn}_5$  (~7 GPa). Cracks were only observed on  $\text{Cu}_6\text{Sn}_5$ , which had a fracture toughness around 0.71 MPa $\sqrt{\text{m}}$ . Anomalous multiple pop-in events were mainly observed on  $\text{Cu}_6\text{Sn}_5$  at strain rates up to 0.1 s<sup>-1</sup> during the loading period of the nanoindentation test. It is presumed that multiple pop-in events in  $\text{Cu}_6\text{Sn}_5$  correlated with the crystallographic characteristics of specific intermetallic compounds.

© 2014 Elsevier B.V. All rights reserved.

## 1. Introduction

Recently, lead-free Sn-based solder bumps have been developed in consideration of environmental issues. High Sn content leads to the formation of  $\text{Cu}_6\text{Sn}_5$  and  $\text{Cu}_3\text{Sn}$  binary intermetallic compounds (IMCs) during the heat-reflow process on the interface between solder bumps and bonding pads (Cu/Ni pads). IMCs formed during the heat-reflow process could improve adhesion between pads and solders via the pegging effect, but brittleness of IMCs may cause them to act as crack initiation sites. Abnormally grown IMCs can dramatically decrease adhesion strength and act as an origin of failure for products. However, IMCs formed at the interface between solder bumps and Cu/Ni pads are localized with small volumes, making it difficult to understand their mechanical behavior. Instrumented indentation (usually called nanoindentation) system are useful for measuring the mechanical behavior of small volumes such as integrated circuits and other systems with dimensions on a micro/nanoscale [1,2]. In this study, we also used

nanoindentation to measure the mechanical properties of small volume IMCs and detected anomalous pop-in events.

During indentation using a wide range of spherical indenter radii, the “pop-in” phenomenon, a sudden jump in the displacement due to the transition from elastic to plastic behavior, was occasionally observed. Pop-in events occurred in several reasons: (1) the shear stress under the indenter tip almost reached the theoretical maximum ( $\sim G/2\pi$ ) for small spheres [3]; (2) Gerberich et al. [4] argued that pop-ins occur also due to fracture during indentation; (3) dislocation interface interactions are suggested as another reason to occur pop-ins shown in work of Aifantis et al. [5].

The frequency of the occurrence of pop-in events decreased with increasing indenter radius [3]. In a similar manner, some materials, such as bulk metallic glasses, e.g.  $\text{Pd}_{40}\text{Ni}_{40}\text{P}_{20}$ ,  $\text{Pd}_{40}\text{Cu}_{30}\text{Ni}_{10}\text{P}_{20}$ ,  $\text{Zr}_{65}\text{Al}_{10}\text{Ni}_{10}\text{Cu}_{15}$ ,  $\text{Zr}_{52.5}\text{Al}_{10}\text{Ni}_{14.6}\text{Cu}_{17.9}\text{Ti}_5$ , presented serrated pop-in events [6,7]. It is known that shear bands formation can cause a transition from elastic to plastic deformation depending upon strain rate. It is also known that the ‘multiple’ pop-in events in amorphous materials like bulk metallic glasses due to shear bands formation is not present in most crystalline materials. A few crystalline materials, like single crystal gold, have ‘multiple’ pop-in events [8] that can be explained by the nucleation–multiplication of

\* Corresponding author at: Department of Cogno-Mechatronics Engineering, Pusan National University, Busan 609-735, Republic of Korea.

E-mail address: [dlee@pusan.ac.kr](mailto:dlee@pusan.ac.kr) (D. Lee).

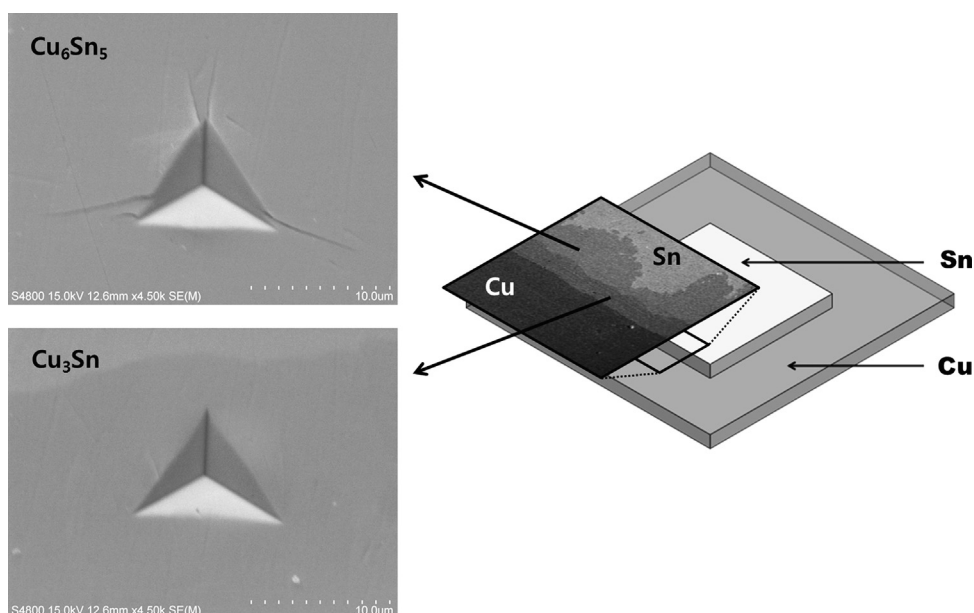


**Fig. 1.** Schematic diagram of diffusion and images of IMC structures after annealing the Cu and Sn plates. A schematic diagram of the diffusion model for the high purity Cu and Sn plates (right), while figures on upper-left and lower-left show the indentations in  $\text{Cu}_6\text{Sn}_5$  and  $\text{Cu}_3\text{Sn}$  respectively.

dislocations. Interestingly, Yang et al. [9] and Xu et al. [10] also reported ‘multiple’ pop-in events in  $\text{Cu}_6\text{Sn}_5$ , which is known as brittle materials due to having fewer slip systems. However, there was no clear explanation regarding this phenomenon in those papers because they were not focused on multiple pop-in events.

We would like to suggest a possible reason for the appearance of serrated pop-in events in IMCs because they occurred on  $\text{Cu}_6\text{Sn}_5$ , which is an IMC.

## 2. Experimental procedure

$\text{Cu}_3\text{Sn}$ ,  $\text{Cu}_6\text{Sn}_5$  IMCs were fabricated using a diffusion process involving bulk Cu–Sn plate at 325 °C in Ar for 48 h. As shown in Fig. 1, the diffusion couple was prepared using a high purity Cu plate (20 mm × 20 mm × 1 mm, 99.99%, Alfa Aesar) and Sn plate (10 mm × 10 mm × 1 mm, 99.9985%, Alfa Aesar). After mechanical polishing, the Cu and Sn plates were chemically polished in 30 vol % of nitric acid and 37 vol% of hydrochloric acid, respectively. The plates were coupled together and tightly bonded with soda-lime glass followed by a heat-treatment in a quartz tube. The annealed diffusion couple was then mechanically polished using diamond paste up to 0.25 μm followed by 0.05 μm alumina powder. The microstructures and chemical compositions of the IMCs were observed using a field-emission scanning electron microscope (FE-SEM, S-4800, Hitachi, Japan) capable of performing energy dispersive x-ray spectrometry (EDS).

Mechanical properties of the IMCs were evaluated using an instrumented indentation technique called nanoindentation (Nanoindenter G200™, Agilent Technologies, USA). Nanoindentation experiments were performed on  $\text{Cu}_3\text{Sn}$  and  $\text{Cu}_6\text{Sn}_5$  using a Berkovich indenter, a three-sided pyramid with triangular faces [11], and the specimens were indented up to 500 nm in depth with strain rates between 0.01 and 1 s<sup>-1</sup>, to observe pop-in events. To observe fracture toughness, the depth of indentation was increased up to 2 μm into the surface. All tests were conducted at room temperature with more than thirty indents for each sample. Two selected indents with strain rates of 0.01 s<sup>-1</sup> and 1 s<sup>-1</sup> on  $\text{Cu}_6\text{Sn}_5$  were cut into 10 μm × 10 μm × 50 nm sections using a focused ion beam (FIB, Dual Beam Focused Ion Beam

**Table 1**  
Chemical composition of IMCs after annealing.

Material	Element	Weight%	Atomic%
$\text{Cu}_3\text{Sn}$	Cu K	58.13	72.17
	Sn L	41.87	27.83
$\text{Cu}_6\text{Sn}_5$	Cu K	37.29	52.63
	Sn L	62.71	47.37

(DB-FIB), Helios NanoLab™, FEI Netherlands) for transmission electron microscopic examination (FE-TEM, JEM-2100F HR, JEOL) to understand detailed microstructural changes caused by indentation strain rate. The elastic modulus and hardness were measured using the Oliver–Pharr method [12,13]. The ANSYS® simulation package (ANSYS 14.0) was used to perform the finite element method to determine the maximum resolved shear stresses at the first pop-in load.

## 3. Results and discussion

As shown in SEM images and a schematic in Fig. 1,  $\text{Cu}_6\text{Sn}_5$  was unevenly formed on the Sn plate side whereas a continuous layer of  $\text{Cu}_3\text{Sn}$  was formed on the Cu plate side. It is presumed that a relatively thin layer of  $\text{Cu}_3\text{Sn}$  first formed on the Cu plate side, and then  $\text{Cu}_6\text{Sn}_5$  grew into the Sn plate side by preferential diffusion through grain boundaries [14]. Chemical compositions were confirmed using EDS analyses (Table 1):  $\text{Cu}_3\text{Sn}$  ( $\text{Cu}_{72.17}\text{Sn}_{27.83}$  in at%), and  $\text{Cu}_6\text{Sn}_5$  ( $\text{Cu}_{52.63}\text{Sn}_{47.37}$  in at%). Both structures were thick enough to do nanoindentation tests, as shown in Fig. 1, and these tests were performed with various conditions. Especially in high load, while cracks around indents on  $\text{Cu}_6\text{Sn}_5$  (upper-left in Fig. 1) were clearly observed, no clear evidence of cracks was detected around indents on  $\text{Cu}_3\text{Sn}$  (lower-left in Fig. 1). Cracks around indents on Cu–Sn intermetallics were reported in other studies [15,16], and based upon the cracking phenomenon fracture toughness is discussed later in this paper.

The Young’s modulus and hardness of  $\text{Cu}_6\text{Sn}_5$  and  $\text{Cu}_3\text{Sn}$  with various strain rates are presented in Table 2. Literature values (published theoretical and experimental data) of conventional

strain rates ( $0.05 \text{ s}^{-1}$ ) are in agreement with this study [9,17]. The modulus and hardness values apparently increased with strain rate: the faster the strain rate, the higher modulus and hardness values observed. Intriguingly, we may infer that  $\text{Cu}_6\text{Sn}_5$  and  $\text{Cu}_3\text{Sn}$  IMCs are highly strain rate sensitive materials at room temperature. It is also argued later in this paper.

As mentioned previously, the indentation strain rate was changed from  $0.01 \text{ s}^{-1}$  to  $1 \text{ s}^{-1}$ , and pop-in events were only observed on  $\text{Cu}_6\text{Sn}_5$  with strain rates up to  $0.1 \text{ s}^{-1}$ , disappearing for increasing strain rate. The same phenomenon was not observed in  $\text{Cu}_3\text{Sn}$ , shown in Fig. 2. The suggested mechanism of pop-in events in the literature is the transition from elastic to elastic–plastic behavior. This transition can be classified in two subcategories: (1) elastic–plastic transition by dislocation nucleation at maximum shear stress [7], (2) shear bands by localized strain. Pop-in events in crystalline materials like  $\text{Al}_2\text{O}_3$ ,  $\text{SiC}$  [18],  $\text{Cr}_3\text{Si}$  [19], and Au single crystals [8] are related to dislocation nucleation at maximum shear stress when purely elastic deformation transformed into elastic–plastic deformation. Shear bands formation could be the most favorable mechanism causing the pop-in phenomenon in non-crystalline materials such as metallic glasses, e.g.  $\text{Pd}_{40}\text{Ni}_{40}\text{P}_{20}$ ,  $\text{Pd}_{40}\text{Cu}_{30}\text{Ni}_{10}\text{P}_{20}$ ,  $\text{Zr}_{65}\text{Al}_{10}\text{Ni}_{10}\text{Cu}_{15}$ ,  $\text{Zr}_{52.5}\text{Al}_{10}\text{Ni}_{14.6}\text{Cu}_{17.9}\text{Ti}_5$  [6,20], and  $\text{Mg}_{65}\text{Cu}_{25}\text{Gd}_{10}$  [21]. However, in some compound semiconductors, e.g.,  $\text{InP}$ ,  $\text{GaN}$ ,  $\text{ZnO}$ , and  $\text{GaAs}$  [22,23], shear bands formation considered a main mechanism of plastic deformation in the pop-in phenomenon.

It is worth to note that most of crystalline materials show a ‘single’ pop-in event which was occasionally reported. On the other hand, non-crystalline or amorphous materials such as bulk metallic glasses and polymers show ‘multiple’ pop-in due to

periodic movement of shear bands under critical pressure. However, a few studies reported ‘multiple’ pop-in events in crystalline materials, single crystal Au [8], and Cu–Sn IMC systems [9,10,24]. Corcoran et al. [8] reported that multiple pop-in events in the Au single crystal are related to the continuous “single generation of dislocation and pile-up process.” The continuous procedure would create parallel slip bands that act like shear bands in amorphous materials. Yang et al. [9] reported the same observation, and argued that multiple pop-in events in  $\text{Cu}_6\text{Sn}_5$  intermetallics could be explained in the same way as those in single crystal Au [8]. However, because IMCs have limited slip systems and high critical resolved shear stress [24], one cannot simply conclude that the mechanism of ‘multiple’ pop-in events is comparable to metallic materials such as Au. As mentioned in Introduction section, another possible mechanism of multiple pop-ins are due to fracture during indentation suggested by Gerberich et al. [4] because several cracks observed around indents shown in Fig. 1 (upper left).

It is worth noting that Yang et al. did not report any ‘multiple’ pop-in events on  $\text{Cu}_3\text{Sn}$  [9], but Xu and Pang [10] presented a load–displacement curve for  $\text{Cu}_3\text{Sn}$  clearly showing ‘multiple’ pop-in events in  $\text{Cu}_3\text{Sn}$ . However, Xu and Pang did not comment on them beyond this. We also could not observe the ‘multiple’ pop-in phenomenon on  $\text{Cu}_3\text{Sn}$  on all strain rates range performed in this study, but very small displacement bursts or relatively non-smooth loading curves on  $\text{Cu}_3\text{Sn}$  were detected under the strain rate of  $0.05 \text{ s}^{-1}$ .

We conjecture that the different mechanical behaviors of  $\text{Cu}_6\text{Sn}_5$  and  $\text{Cu}_3\text{Sn}$  may be related to crystal structure.  $\text{Cu}_3\text{Sn}$  has a long-range ordered orthorhombic crystal structure that is composed of twelve Cu atoms around a Sn atom [25]. On the other hand, Cu and Sn atom in  $\text{Cu}_6\text{Sn}_5$  are surrounded by six Sn atoms and six Cu atoms, respectively, and  $\text{Cu}_6\text{Sn}_5$  is hexagonal around  $200 \text{ }^\circ\text{C}$  and monoclinic at lower temperatures [26,27]. The crystal volume change of hexagonal to monoclinic  $\text{Cu}_6\text{Sn}_5$  is about 2.15%, which could create internal residual stress. Jiang and Chawla [24] observed “multiple-strain-burst” such as ‘multiple’ pop-ins in  $\text{Cu}_6\text{Sn}_5$  pillars fabricated by FIB followed by pressing with flat-punch indenter. They argued that the multiple-strain-burst was due to cleavage fracture along certain crystallographic planes. Subsequently, crystal structure and relatively large residual stress may promote dislocation movement and/or slip plane cleavage.

Cracks were only generated during indentation at the end of the indent tip at a  $\sim 130 \text{ mN}$  load on  $\text{Cu}_6\text{Sn}_5$ , shown in Fig.1a. The fracture toughness,  $K_{IC}$ , of  $\text{Cu}_6\text{Sn}_5$  was calculated using the

**Table 2**  
Young’s Modulus and Hardness of IMCs.

Specimen	Strain rate ( $\text{S}^{-1}$ )	E Modulus (GPa)	Hardness (GPa)
$\text{Cu}_3\text{Sn}$	0.01	$110.02 \pm 14.88$	$5.36 \pm 0.93$
	0.05	$140.83 \pm 7.46$	$6.17 \pm 0.19$
	0.1	$149.50 \pm 11.41$	$6.66 \pm 0.24$
	0.5	$151.39 \pm 9.88$	$6.84 \pm 0.19$
	1	$154.55 \pm 7.96$	$9.54 \pm 0.71$
$\text{Cu}_6\text{Sn}_5$	0.01	$98.01 \pm 8.5$	$6.47 \pm 0.93$
	0.05	$124.99 \pm 1.46$	$6.96 \pm 0.06$
	0.1	$126.25 \pm 1.30$	$7.27 \pm 0.031$
	0.5	$127.93 \pm 1.98$	$7.55 \pm 0.11$
	1	$133.20 \pm 9.745$	$12.20 \pm 0.87$

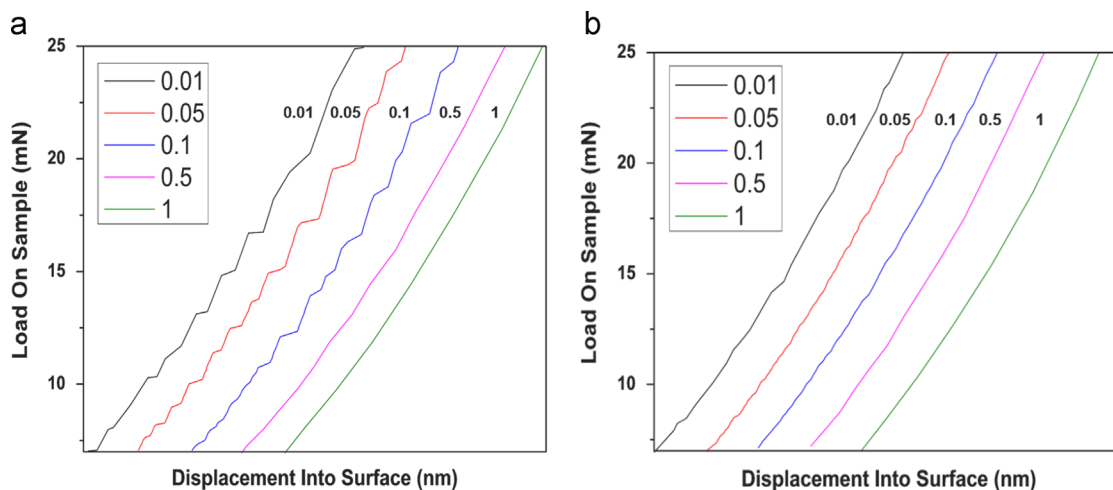


**Fig. 2.** Indentation curves following strain rate, offset by 100 nm. (a)  $\text{Cu}_6\text{Sn}_5$ , (b)  $\text{Cu}_3\text{Sn}$ .

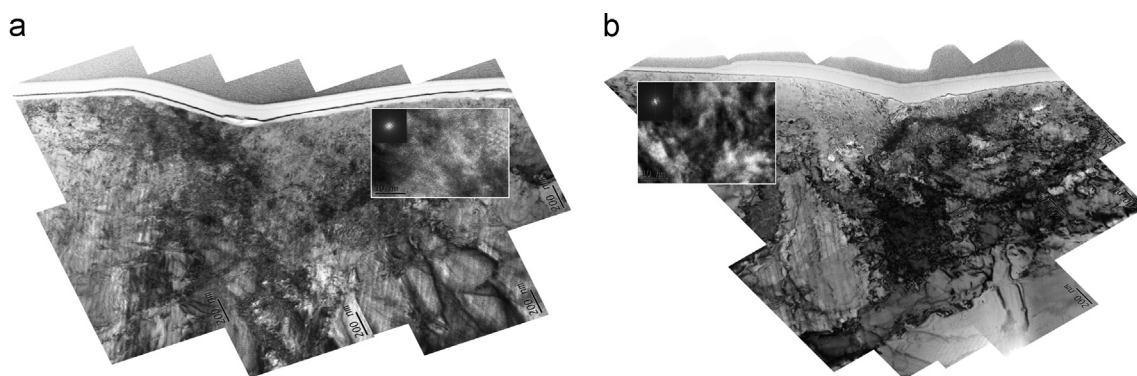


**Fig. 3.** FE-TEM images of a  $\text{Cu}_6\text{Sn}_5$  cross section. Cross-sections were made at strain rates of (a)  $0.01 \text{ s}^{-1}$ , and (b)  $1 \text{ s}^{-1}$ .

following equation [15]:

$$K_C = \alpha \left( \frac{E}{H} \right)^{1/2} \times \left( \frac{P_{max}}{C^{3/2}} \right) \quad (1)$$

where  $P_{max}$  is the maximum indentation load,  $C$  is crack length,  $E$  is the Young's modulus,  $H$  is the hardness, and  $\alpha$  is an empirical constant which depends on geometry of the indenter tip ( $\alpha=0.016$  for a Berkovich tip). Based on the results, fracture toughness was about  $0.71 \text{ MPa}\sqrt{\text{m}}$ , which is similar to silicon and soda-lime glass [28]. Cracks were not observed on  $\text{Cu}_3\text{Sn}$  in Fig.1b. Presumably, the cracking characteristics of  $\text{Cu}_6\text{Sn}_5$  under the applied load in this study could also be related to crystal structure and phase-transformation induced residual stress.

TEM samples were made by cross-sectioning  $\text{Cu}_6\text{Sn}_5$  indents using an FIB to observe how strain rate affected the microstructures under the indent. Fig. 3 shows the TEM images. Fig. 3a and b shows TEM images of the specimens indented with strain rates of  $0.01 \text{ s}^{-1}$  and  $1 \text{ s}^{-1}$ , respectively. The widespread dark-region is clearly observed with increasing strain rate. The darker contrasting region could be related to dislocation tangling or slip regimes. We assume the dark region is closely connected to the dislocation velocity expressed in Eq. 2. In Eq. 2, the dislocation velocity is proportional to the shear stress applied on the specimen by the power law relation:

$$v = A\tau^m \quad (2)$$

where  $A$  is material constant,  $m$  is approximately 1 at 300 K in pure crystal and increases to 2–5 with alloying, and  $\tau$  is shear stress [29]. We calculated the critical resolved shear stress,  $\tau$ , using the commercial finite element method program ANSYS<sup>®</sup>.  $\tau$  was about 24% higher at a strain rate of  $1 \text{ s}^{-1}$  than one of  $0.01 \text{ s}^{-1}$ . Therefore, dislocation velocity under indents with higher strain rates could be much faster and cause dislocation tangling. 'Multiple' pop-in events are caused by repetition of the transformation of purely elastic deformation to plastic–elastic deformation that is easily seen at lower strain rates. However, the dislocation velocity increased with shear stress in faster strain rate tests, thus the deformation speed also increased. Therefore, a nanoindentation system may not have detected this due to significantly shorter time to next movement. Phenomenologically, brittle IMC,  $\text{Cu}_6\text{Sn}_5$  ( $K_C \sim 0.71 \text{ MPa}\sqrt{\text{m}}$ ), presented 'multiple' pop-in phenomenon and strain rate sensitive behavior. With this observation, we speculate that a few dislocations in  $\text{Cu}_6\text{Sn}_5$  might move along the specific crystallographic directions, which will be act as cleavage fracture on higher load, and those are accumulated by strained crystalline regime caused by phase transformation. Due to multiple steps of these procedures, we might observe 'multiple' pop-in events even in intermetallic compounds, specifically  $\text{Cu}_6\text{Sn}_5$ .

#### 4. Conclusions

To understand the mechanical characteristics of Cu–Sn-based IMCs, a Cu–Sn diffusion couple was prepared and annealed at  $325 \text{ }^\circ\text{C}$  for 48 h in an Ar atmosphere in a quartz tube furnace.  $\text{Cu}_6\text{Sn}_5$  and  $\text{Cu}_3\text{Sn}$  IMCs were mainly observed, which grew at the interface of Cu–Sn diffusion couple around  $100 \text{ }\mu\text{m}$  and  $40 \text{ }\mu\text{m}$ , respectively. For examining the mechanical behavior of IMCs, we used a nanoindentation system. Young's Modulus of  $\text{Cu}_3\text{Sn}$  ( $\sim 125 \text{ GPa}$ ) was about 12% higher than that of  $\text{Cu}_6\text{Sn}_5$  ( $\sim 125 \text{ GPa}$ ) in  $0.05 \text{ s}^{-1}$ , but hardness of  $\text{Cu}_3\text{Sn}$  ( $\sim 6 \text{ GPa}$ ) was about 15% lower than that of  $\text{Cu}_6\text{Sn}_5$  ( $\sim 7 \text{ GPa}$ ). IMC fracture toughness was calculated based upon cracks formed around indents. We only observed cracks around indents on  $\text{Cu}_6\text{Sn}_5$ , and its fracture toughness was about  $0.71 \text{ MPa}\sqrt{\text{m}}$ . Even though  $\text{Cu}_6\text{Sn}_5$  is a highly brittle material, 'multiple' pop-in events during the loading period of the nanoindentation test were mainly observed at strain rates up to  $0.1 \text{ s}^{-1}$ . 'Multiple' pop-in events were not detected as the strain rate increased. As a result, it is presumed that the 'multiple' pop-in events in  $\text{Cu}_6\text{Sn}_5$  correlated with crystallographic characteristics of specific intermetallic compounds, which are related to dislocation movement, cracking phenomenon, etc. Furthermore, we may need detailed study to understand mechanical properties (including pop-in events) of  $\text{Cu}_3\text{Sn}$  alloy system.

#### Acknowledgments

The authors would like to give special thanks to Professor George M. Pharr at the Department of Materials Science and Engineering, University of Tennessee & Oak Ridge National Laboratory, USA for valuable discussion about multiple pop-in events. This research was co-supported by (1) the Basic Science Research Program through the National Research Foundation of Korea (NRF) funded by the Ministry of Education (NRF-2010-0025175); (2) a grant from the Fundamental R&D Program for Core Technology of Materials funded by the Ministry of Knowledge Economy, Republic of Korea; (3) the Civil & Military Technology Cooperation Program through the National Research Foundation of Korea (NRF) funded by the Ministry of Science, ICT & Future Planning (No. 2013M3C1A9055407).

#### References

- [1] N.X. Randall, E. Hollander, C. Julia-Schmutz, *Surf. Coat. Technol.* 99 (1998) 111–117.
- [2] A. Heryanto, W.N. Putra, A. Trigg, S. Gao, W.S. Kwon, F.X. Che, X.F. Ang, J. Wei, R.I. Made, C.L. Gan, K.L. Pey, *J. Electron. Mater.* 41 (2012) 2533–2542.
- [3] S. Shim, H. Bei, E.P. George, G.M. Pharr, *Scr. Mater.* 59 (2008) 1095–1098.
- [4] W.W. Gerberich, D.E. Kramer, N.I. Tymiak, A.A. Volinsky, D.F. Bahr, M.D. Kriese, *Acta Mater.* 47 (1999) 4115–4123.

- [5] Katerina E. Aifantis, A.H.W. Ngan, *Mater. Sci. Eng. A-Struct.* 59 (2007) 251–261.
- [6] C.A. Schuh, T.G. Nieh, *Acta Mater.* 51 (2003) 87–99.
- [7] J.R. Morris, H. Bei, G.M. Pharr, E.P. George, *Phys. Rev. Lett.* 106 (2011) 165502.
- [8] S.G. Corcoran, R.J. Colton, E.T. Lilleodden, W.W. Gerberich, *Phys. Rev. B* 55 (1997) R16057.
- [9] P.F. Yang, Y.S. Lai, S.R. Jian, J. Chen, R.S. Chen, *Mater. Sci. Eng. A-Struct.* 485 (2008) 305–310.
- [10] L. Xu, J.H.L. Pang, *Thin Solid Films* 504 (2006) 362–366.
- [11] M.M. Khrushchov, E.S. Berkovich, *Ind. Diam. Rev.* 11 (1951) 42–49.
- [12] W.C. Oliver, G.M. Pharr, *J. Mater. Res.* 7 (1992) 1564–1583.
- [13] W.C. Oliver, G.M. Pharr, *J. Mater. Res.* 19 (2004) 3–20.
- [14] P. Shewmon, *Diffusion in Solids*, second ed., TMS, Pennsylvania, 1989.
- [15] G. Ghosh, *J. Mater. Res.* 19 (2004) 1439–1454.
- [16] J.S. Kang, R.A. Gagliano, G. Ghosh, M.E. Fine, *J. Electron. Mater.* 31 (2002) 1238–1243.
- [17] H.C. Cheng, C.F. Yu, W.H. Chen, *J. Mater. Sci.* 47 (2012) 3103–3114.
- [18] T.F. Page, W.C. Oliver, C.J. McHargue, *J. Mater. Res.* (1992) 450–473.
- [19] H. Bei, E.P. George, J.L. Hay, G.M. Pharr, *Phys. Rev. Lett.* 95 (2005) 45501.
- [20] C.A. Schuh, T.G. Nieh, *J. Mater. Res.* 19 (2004) 46–57.
- [21] C.A. Schuh, T.G. Nieh, *Acta Mater.* 52 (2004) 5879–5891.
- [22] J.E. Bradby, J.S. Williams, J. Wong-Leung, M.V. Swain, P. Munroe, *Appl. Phys. Lett.* 78 (2001) 3235–3237.
- [23] J.E. Bradby, J.S. Williams, M.V. Swain, *J. Mater. Res.* 19 (2004) 380–386.
- [24] L. Jiang, N. Chawla, *Scr. Mater.* 63 (2010) 480–483.
- [25] A. Paul, C. Ghosh, W.J. Boettinger, *Metall. Mater. Trans. A* 42 (2011) 952–963.
- [26] A. Gangulee, G.C. Das, M.B. Bever, *Metall. Mater. Trans. B* 4 (1973) 2063–2066.
- [27] K. Nogita, C.M. Gourlay, T. Nishimura, *JOM* 61 (2009) 45–51.
- [28] G.R. Anstis, P. Chantikul, B.R. Lawn, D.B. Marshall, *J. Am. Ceram. Soc.* 64 (2006) 533–538.
- [29] D. Hull, D.J. Bacon, *Introduction to Dislocations*, third ed, Butterworth-Heinemann, Liverpool, 1984.